Jour. Korean Inst. Mining Geol.
Vol.21, No.1, p. 107-113, 1988

Two-Dimensional Inversion for Dipole-Dipole Resistivity Data

Hee Joon Kim* and Younghwa Kim**

Abstract : We present a precedure for interpreting dipole-dipole apparent resistivity data. The procedure is constructed by combining a forward two-dimensional finite element modeling and an inverse technique with Householder's transformation. In the interpretation, subsurface structure is divided into some blocks with constant resistivities. Our inversion technique is tested on synthetic and field data. We found that geologic constraint is required for successful interpretation.

INTRODUCTION

In regions such as sedimentary basins where the lateral variation of structure is slow, good regional interpretation can be made by fitting layered one dimensional (1D) earth models. However, in many cases, such as mineral and geothermal explorations, 1D models are not applicable. A more general interpretation assumes that regional resistivity varies little in one direction, the "strike" direction. This is the two-dimensional (2D) problem.

With the development of numerical methods and large computers, trial-and-error forward modeling has been used extensively to interpret data in term of complex 2D earth models. The trial-and-error method, however, is difficult and time consuming, and gives little information about model resolution. To make interpretation easier and more objective, a non-linear 2D inversion technique is needed to determine the subsurface structure.

Solutions for the inverse problem in the electrical resistivity method was firstly found by Pelton et al. (1978), but their method needs too many constraints. The three-dimensional (3D) resistivity inversion using alpha center developed by Petrick et al. (1981) may determine the positions of conductivity inhomogeneities, but it cannot determine their sizes or conductivities. More general 2D inversion methods were developed by Sasaki (1981), Smith and Vozoff (1984), and Tripp et al (1984). Main differences among their methods are forward modeling techniques employed. Sasaki (1981) used the finited element method, Smith and Vozoff (1984) used the finite difference method, and Tripp et al. (1984) used the transmission-surface analogy method.

In this paper, 2D inversion method for interpreting dipole-dipole resistivity data is made by combining finite element forward modeling technique (Kim, 1986) and inverse technique with Householder's transformation (Kim, 1985). The 2D inversion method is tested on synthetic and field data. The field date used in this paper was collected in the Yangsan fault area (Kim, 1987). Influences of initial guess, number of data points, number of blocks with constant resistivities, and gelogic information on the inversion method are discussed in this paper.

NUMERICAL FORMULATION

Forward Problem

The forward problem consists of producing a set of model apparent resistivity data as would be found by given electrode arrays on a line in

* Department of Applied Geology, National Fisheries University of Pusan
* * Department of Geology, Kangwon National University

the x direction(perpendicular to "strike") on the surface of a halfspace. In this paper, finite element method (Kim, 1986) is used to evaluate the potential in the (x,z)-plane from the generalized Poisson's equation

$$-\nabla \cdot [\sigma(x,z)\nabla \phi(x,y,z)] = \frac{\partial \rho}{\partial t}\delta(x_s)\delta(y_s)\delta(z_s), \quad (1)$$

where σ is the conductivity, ϕ the potential, ρ the charge density specified at a point by the Dirac delta function δ, and (x_s,y_s,z_s) the coordinates of the point source. The first term in (1) contains $\sigma(x,z)$ instead of $\sigma(x,y,z)$ because it is assumed that there is no change in conductivity in the y direction (2D assumption).

The solution is carried out for a set of λ values in Fourier space and an inverse Fourier transform is employed to return $\phi(x,y,z)$ from a set of Fourier transformed potential $\tilde{\phi}(x, \lambda, z)$. In the Fourier space, (1) becomes, for each value of λ,

$$-\nabla \cdot [\sigma(x,y)\nabla \tilde{\phi}(x,\lambda,z)] + \lambda^2 \sigma(x,z)\tilde{\phi}(z,\lambda,z) = \tilde{Q}(x_s)\delta(z_s) \quad (2)$$

where $\tilde{Q}$, the steady-state current density in λ space, is related to current J injected at a point (x_s,z_s) by

$$\tilde{Q} = J/(2\triangle A),$$

where $\triangle A$ is a small area about the injection point.

Under an appropriate boundary condition, (2) can be solved numerically by the finite element method. In this process, the set of simultaneous equations for all modes may be expressed in matrix form

$$[C] \cdot [\tilde{\phi}] = [S], \quad (3)$$

where [C] is the bounded matrix whose terms depend on the 2D conductivity structure and on the transform variable λ, $[\tilde{\phi}]$ is the vector of transformed potential, and [S] is the vector of source current in the transformed domain. An inverse Fourier transformation returns ϕ from $\tilde{\phi}$, and an apparent resistivity ρ_a can be calculated by

$$\rho_a = G\triangle\phi/J,$$

where G is the geometric factor dependent on the array used, and $\triangle\phi$ is the potential difference between two electrodes.

Partial Derivative

In the inversion process described later, partial derivatives of ρ_a with respect to model conductivity should be evaluated. In practice, the 2D conductivity structure is divided into some blocks with a constant conductivity. For a set of apparent resistivities, partial derivatives with respect to the set of block conductivities, $[\partial \rho_a/\partial \sigma_B]$, are calculated from $[\partial \phi/\partial \sigma_B]$.

Partial differentiation of (3) yields

$$\left[\frac{\partial C}{\partial \sigma_B}\right][\tilde{\phi}] + [C]\left[\frac{\partial \tilde{\phi}}{\partial \sigma_B}\right] = 0,$$

so that

$$[C]\left[\frac{\partial \tilde{\phi}}{\partial \sigma_B}\right] = -\left[\frac{\partial C}{\partial \sigma_B}\right][\tilde{\phi}] \quad (4)$$

This equation is exactly analogous to (3). Thus the same procedure used to solve (3) for $[\tilde{\phi}]$ is available to solve (4) for $[\partial \tilde{\phi}/\partial \sigma_B]$. Inverse Fourier transformation of $\partial \tilde{\phi}/\partial \sigma_B$ yields $\partial \tilde{\phi}/\partial \sigma_B$ from which $\partial \rho_a/\partial \sigma_B$ is calculated.

Inverse Problem

The inverse problem is solved by using the procedure described by Kim (1986). For completeness, a brief summary of the procedure is given in this section.

Since apparent resistivity ρ_a and block resistivity ρ_B (model parameter) are positive values, a logarithmic transformation of them is useful in the inversion (Rijo et al., 1977). After transforming to logarithmic apparent resistivities F and logarithmic parameters P, an approximate linear expression relating in F and P is

$$\triangle F = A\triangle P + R \quad (5)$$

where $\triangle F$ and $\triangle P$ are the vectors of the

changes in F and P, respectively, R the residual vector, and A the Jacobian matrix of derivatives with respect to parameters:

$$a_{ij}=\frac{\partial f_i}{\partial p_i}\Big| P_0, \quad (6)$$

where P_0 is the initial guess. A stable least-squares solution may be obtained from an equation (Marquardt, 1963)

$$(A^TA+v^2I)\triangle P=A^T\triangle F, \quad (7)$$

where I is the identity matrix and v^2 is a certain positive value.

In order to use the Householder's transformation, we must return to the obsevation equation (5). The least-squares problem equivalent to (6) can be written as

$$\begin{bmatrix}\triangle F\\ O\end{bmatrix}=\begin{bmatrix}A\\ v\end{bmatrix}\triangle P+\begin{bmatrix}R\\ O\end{bmatrix}$$

This equation is solved by Householder's transforming $[A,vI]^T$, and it is known that its solution is usually stable numerically (Kim, 1986).

A procedure which carefully selects an appropriate value for v^2 at each interation in the inversion process is called ridge regression method (Marquardt, 1963). In this paper, however, we fix v^2 to a constant value throughout the inversion process. Some merits of the constant v^2 can be found in Sasaki (1984).

PRACTICAL INVERSION

Synthetic Data

In determining the behavior of a particular inversion algorithm, it is important to apply the algorithm to synthetic data corresponding to a model with known parmeters. The 2D earth model considered in this paper is shown in Fig. 1. The 2D earth consists of a vertical contact of two regions of 40 and 100 Ω · m, and a small conductive body of 10 Ω · m which is imbedded in the region of 100 Ω · m. Fig. 2 shows apparent resistivity pseudosection for a dipole-dipole array perpendicular to the strike of the 2D earth. The synthetic data is made by adding 5% random Gaussian noise to the apparent resistivities computed by the finite element method with 80x 16 meshs.

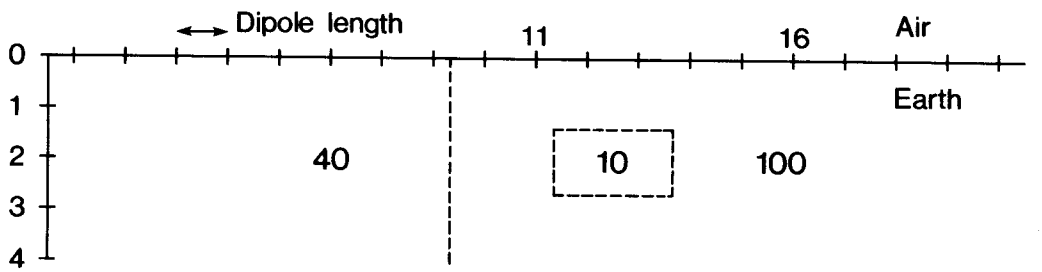

Fig. 1 2D earth model.

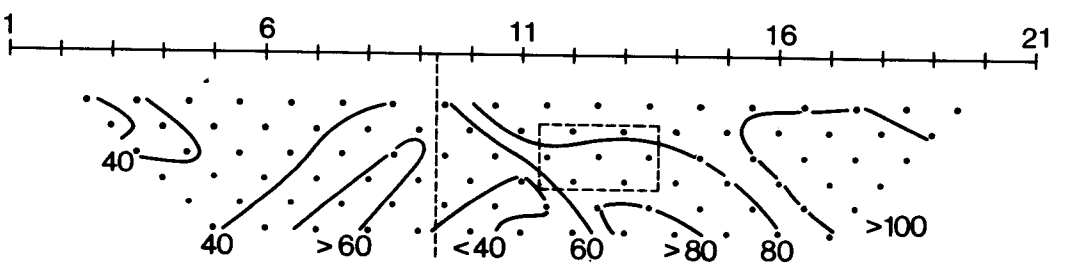

Fig. 2 Dipole-dipole apparent resistivity pseudosection. Units are in Ω · m. Contour interval is 20 m.

Using the synthetic data, inversion tests are made for four cases. A 2D earth with 30 blocks shown in Fig. 3 is used for the cases 1 and 2. In the case 1, full data set with 93 apparent resistivities, which are obtained for electrodes 1 to 21 and for dipole spacings (n) 1 to 6, are used in the resistivity inversion. In the case 2, reduced data set with 60 apparent resistivities, which are computed for eledtrodes 3 to 19 and n=1 to 5, are used. A 2D earth with 35 blocks shown in Fig. 4 is used for the case 3. Some geologic informations may be useful for a better inversion analysis. Fig. 5 shows a 2D earth with 30 blocks used for the case 4, and the position of the vertical contact shown in Fig. 1 is reflected in determining the positions and sizes of blocks.

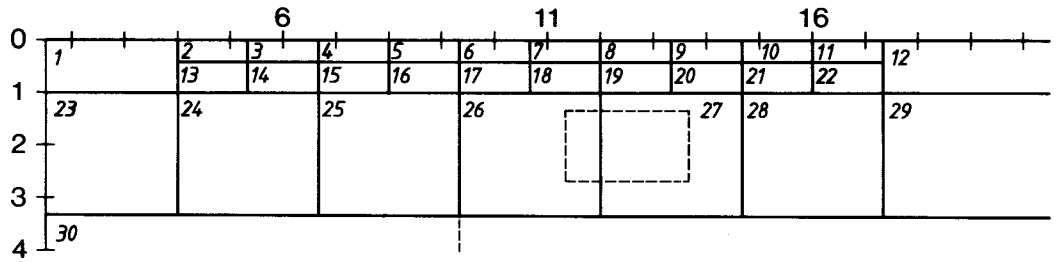

Fig. 3 2D earth model with 30 blocks.

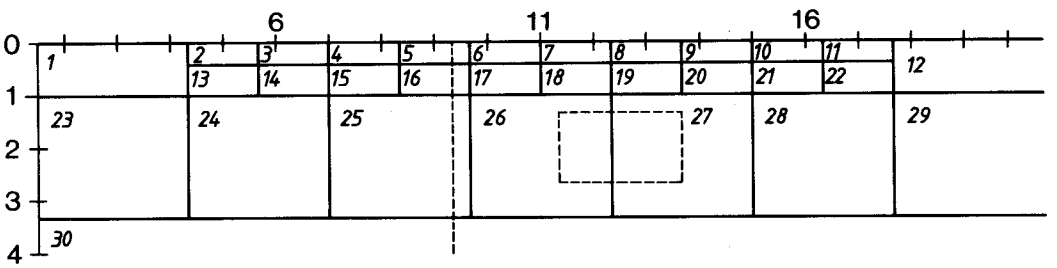

Fig. 4 2D earth model with 35 blocks.

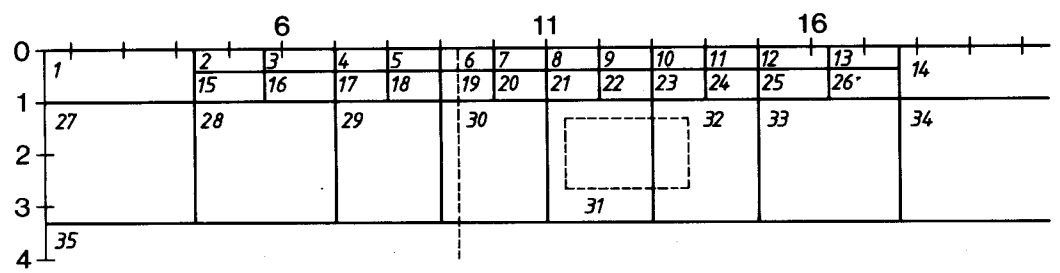

Fig. 5 2D earth model with 30 blocks. The position of vertical contact is reflected in the block structure.

Table 1 lists results of inversion test after 10 iterations for the case 1, 2, 3 and 4. In all of the inversion tests, the Marquardt number v^2 is fixed to 0.01. Fig. 6 shows convergences of root-mean-square (RMS) residual error for each case. After 5 or 6 iterations each RMS residual error reaches to a convergence. The RMS errors for the cases 3 and 4 drop below the added noise level of 5% after more than 4 iterations, whereas those for the cases 1 and 2 are higher than the noise level even after 10 iterations.

Table 1 Results of 2D resistivity inversion for four cases. BR : block resistivity (Ω·m), ESD : estimated standard deviation (%), and RMSE : RMS error.

	Case 1		Case 2		Case 3		Case 4	
No.	BR	ESD	BR	ESD	BR	ESD	BR	ESD
1	39	6	33	23	39	3	40	4
2	33	10	32	17	34	6	39	6
3	49	12	50	15	44	8	38	10
4	78	14	85	18	46	8	31	7
5	247	49	126	38	89	15	33	7
6	77	6	68	6	137	11	80	6
7	86	8	72	7	89	6	106	6
8	70	7	69	9	88	5	100	5
9	75	7	100	16	90	5	87	5
10	102	11	149	25	101	6	118	7
11	1,091	216	936	237	107	6	154	10
12	103	6	196	64	125	9	100	3
13	54	19	54	47	176	18	43	10
14	34	11	35	14	101	3	39	14
15	23	9	21	10	49	11	46	10
16	20	13	22	15	35	8	45	9
17	282	18	290	24	46	9	156	12
18	88	12	112	13	23	9	90	7
19	116	14	120	17	46	6	97	7
20	163	14	113	19	122	9	166	10
21	78	9	69	22	123	10	82	6
22	42	15	30	34	111	10	63	7
23	40	15	95	1,000	98	10	40	12
24	32	15	32	21	113	8	37	13
25	93	24	136	47	82	7	38	10
26	45	16	29	25	65	11	63	10
27	33	17	40	24	41	9	31	9
28	306	39	1,632	1,000	33	10	173	12
29	85	14	17	291	42	13	95	7
30	42	25	29	61	135	13	66	19
31					25	14		
32					63	13		
33					148	14		
34					96	9		
35					48	17		
	RMSE=.0721		.0738		.0405		.0460	

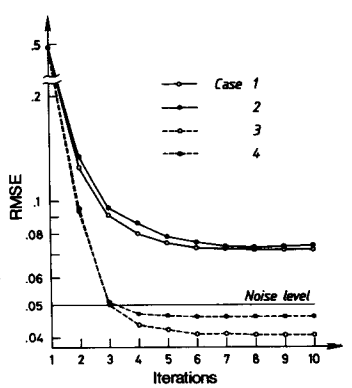

Fig. 6 Convergences of RMS residual errors for the four cases.

The main reason why sufficient convergences below the noise level are not achieved for the cases 1 and 2 is that the block structure shown in Fig. 3 is not suitable for representing the 2D earth shown in Fig. 1. By reducing the sizes of blocks in the vicinity of the vertical contact and the small body, we get a better result as in the case 3. Reflecting the known position of vertical contact to a block structure yields a good result as in the case 4. Estimated standard deviations (ESD) generally increase with a decrase of data to be analyzed as shown in Table 1 (compare the case 1 and 21 the case 2). Since the electrodes 1, 2, 20 and are lost in the case

2, the ESD in blocks 23, 28 and 29 are particularly high.

Field Data

Fig. 7 shows a pseudosectional view of apparent resistivities collected in the Yangsan fault ares (Kim, 1987). These data were produced by dipole-dipole survey with two dipole lengths of 30m and 90m. The survey line cuts across the Yangsan fault in between stations 9 and 10. In the pseudosection, larger values are observed in the western side and smaller values in the eastern side. Unfortunately, insufficient amount of data were provided on account of the heavy traffic condition and the limited range of electrode spacings.

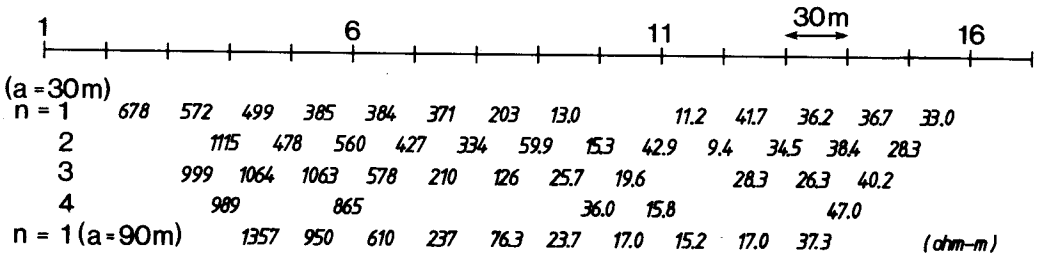

Fig. 7 Dipole-dipole apparent resistivity pseudosection measured in the Yangsan area (Kim, 1987). Dipole length and dipole spacing are shown by a and n, respectively

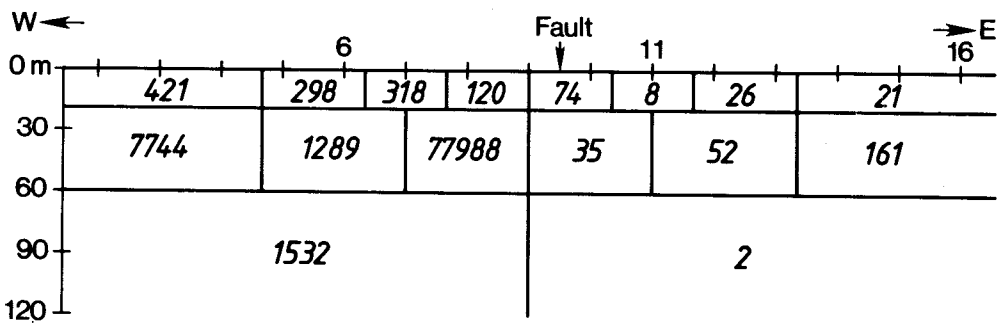

Fig. 8 Resistivity model section with 16 block is inverted by the field data shown in Fig. 7.

Fig. 8 shows a final resistivity model section with 16 blocks inverted by the field data. The model section was obtained after 5 iterations, and RMS error is 38%. The large RMS error seems to be due to near-surface inhomogeneities and 3D effects. The extremely high resistivity of 77988 Ω · m may be caused by a matching of severely contrastive resistivity distribution between both sides of the fault. Fig. 8 yields the following features. The western rigion of the fault reveals larger resistivities than in the eastern region. And the subsurface resistivities increase with depth in the western side of the fault. The fault seems to incline to the west with depth considering that the sharp resistivity boundary can be recognized just below the station 9 in the model section, whereas the surface trace of the fault is confirmed in between stations 9 and 10 as was illustrated by Kim (1987).

CONCLUDING REMARKS

The 2D inversion method described in this paper can be a useful tool in interpreting the result of dipole-dipole resistivity survey. With simple modifications it can treat other arrays. The main limitations of the method are that the geometry of model section must be specified in advance and that it is difficult to determine

whether model misfit is due to 3D effects or to underparameterization in the 2D model. Geologic information is available in support of the data to be inverted, particularly in the choice of initial model and the constraint of inversion. Information on the relative reliability of data points will also help to prevent false conclusion being drawn from coherent error.

ACKNOWLEDGEMENTS

We wish to thank to Dr. K.H. Lee, Seoul Nat'l Univ,. for his helpful comments on this research. We also wish to thank to Drs. D.C. Kim and Y.Q. Kang, Nat'l Fish. Univ. of pusan, for their cardful readings of the manuscript.

REFERENCES

Kim, H.J. (1985) Resistivity inversion with Householder's transformation. J. Korean Inst. Mining Geol., v.18, p. 217-224.

Kim, H.J. (1986) Two-dimensional resistivity modeling by finite element method. J. Korean Inst. Mining Geol., v.19, p. 283-292.

Kim, Y. (1987) A geoelectric study on the structure of the Yangsan fault. Ph.D. dissertation, Seoul Nat'l Univ., 107p.

Marquardt, D.W.(1963) An algorithm for least-squares estimation of nonlinear parameters. J. Soc. Indust. Appl. Math,. v.11, p. 431-441.

Pelton, W.H., Rijo, L., and Swift, C.M., Jr. (1978) Inversion of two dimensional resistivity and induced-polarization data. Geophysics, v.43, p. 485-506.

Petrick, W.R., Sill, W.M., and Ward, S.H. (1981) Three-dimensional resistivity inversion using alpha centers. Geophysics, v.46, p. 1148-1162.

Rijo, L., Pelton, W.H., Feitosa, E.C., and Ward, S.H. (1977) Interpretation of apparent resistivity data from Apodi valley, Rio Grande do Norte, Brazil, Geophysics, v.42, p.811-822.

Sasaki, Y. (1981) Automatic interpretation of resistivity sounding data over two-dimensional structure (I). Butsuri-Tanko (Geophys. Expl.), v.34, p. 341-350. (in Japanese)

Sasaki, Y. (1984) Accuracy of 2D interpretation of resistivity data (II): Case of dipole-dipole array. Butsuri-Tanko (Geophys. Expl.), v.37, p. 105-114. (in Japanese)

Smith, N.C., and Vozoff, K. (1984) Two-dimensional DC resistivity inversion for dipole-dipole data. IEEE Trans. Geosci. Remote Sensing, v.GE-22, p. 21-28.

Tripp, A.C., Hohmann, G.W., and Swift, C.M., Jr. (1984) Two-dimensional resistivity inversion, Geophysics, v.49, p. 1708-1717.

쌍극자 비저항 데이타에 대한 2차원 역해석

김 희 준·김 영 화

요약 : 쌍극자 배열에 대한 겉보기 비저항 데이타를 해석 할 방법을 소개한다. 이 방법은 유한요소법을 이용한 2차원 전진 모델링 기술과 Householder 변환을 사용한 역전 기술을 결합함으로서 작성되었다. 데이타해석은 지하구조를 일정한 비저항을 가진 몇개의 소영역으로 나누어 수행된다. 본 연구의 역해석 기술은 합성 및 야외 데이타를 이용하여 검토되었고, 성공적인 해석을 위하여 지질학적인 정보가 필수적임을 확인하였다.